Glass Physics and Chemistry, Vol. 31, No. 5, 2005, pp. 661–670.

Temperature Dependence of the Concentration of Silanol Groups in Silica Precipitated from a Hydrothermal Solution

V. V. Potapov* and L. T. Zhuravlev**

** Geotechnological Research Center, Far East Division, Russian Academy of Sciences, Severo-Vostochnoe sh. 30, POB 56, Petropavlovsk-Kamchatskii, 683002 Russia*

*** Institute of Physical Chemistry, Russian Academy of Sciences, Leninskii pr. 31, Moscow, GSP -1, 119991 Russia*

Received August 6, 2004

Abstract—The physicochemical characteristics of amorphous silica precipitated from a hydrothermal solution are investigated. The specific surface of silica is determined by the Brunauer–Emmett–Teller method from the data on low-temperature nitrogen absorption. The limits of the total water content are estimated according to the thermogravimetric data. The temperature dependences of the concentration of surface and internal silanol groups in the range 200–1200°C are determined by comparing the thermogravimetric data with the Zhuravlev physicochemical constants for the silica samples under consideration. A new type of amorphous silica with a considerable concentration of internal water is revealed. It is established that the mechanisms of removal of surface and internal water differ from each other.

INTRODUCTION

A colloidal silica dispersion is formed in a hydrothermal solution through a series of successive physicochemical processes. The initial silica concentration depends on the temperature at which the chemical equilibrium of water and aluminosilicate minerals of rocks is attained in a high-temperature hydrothermal field [1–3]. At temperatures of 250–350°C, the total content C_t of silicon dioxide SiO_2 in water virtually corresponds to the solubility of quartz (500–700 mg/kg). In solutions, silicon predominantly occurs in the monomeric form as H_4SiO_4 orthosilicic acid molecules.

After ascending filtration in rocks or rise to the surface in producing wells of geothermal electric power stations, the solution becomes supersaturated with respect to the solubility C_e of amorphous silica due to the decrease in the pressure and temperature and partial evaporation [3]. In this case, the total silica content C_t in the solution can be as high as 700–1500 mg/kg [3]. The solution supersaturation, which is equal to the difference $(C_s - C_e)$ between the concentration C_s of orthosilicic acid and the solubility C_e, is the driving force of polycondensation of silicic acid molecules with the formation of siloxane bonds and partial dehydration [4]; that is,

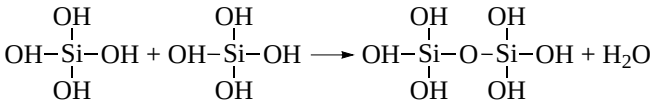

(1)

or

$$Si_mO_{(m-1)}(OH)_{(2m+2)} + Si_nO_{(n-1)}(OH)_{(2n+2)} \longrightarrow Si_{(m+n)}O_{(m+n-1)}OH_{(2n+2m+2)} + H_2O. \quad (2)$$

Nucleation and polycondensation result in the formation of colloidal particles consisting of $nSiO_2 \cdot mH_2O$ hydrated silica in the solution. Surface silanol groups SiOH dissociate with detachment of H^+ protons, and the particle surface acquires a negative electric charge. The electrostatic repulsive forces prevent the particle coagulation and provide the stability of colloidal silica in the hydrothermal solution.

Investigation into the physicochemical characteristics of colloidal silica in the hydrothermal solution and after its precipitation is required to improve a model of formation of minerals in hydrothermal minerals [5, 6], including ore minerals, and to develop a technology of extracting and using silica in order to increase the efficiency of geothermal electric power stations [7].

SAMPLE PREPARATION AND EXPERIMENTAL TECHNIQUE

Silica samples were prepared by freezing a dispersed solution from wells of the Mutnovsk field. On the snow surface, solution drops freeze and colloidal silica particles were clustered in regions between ice crystals. This led to a decrease in the distance between

1087-6596/05/3105-0661

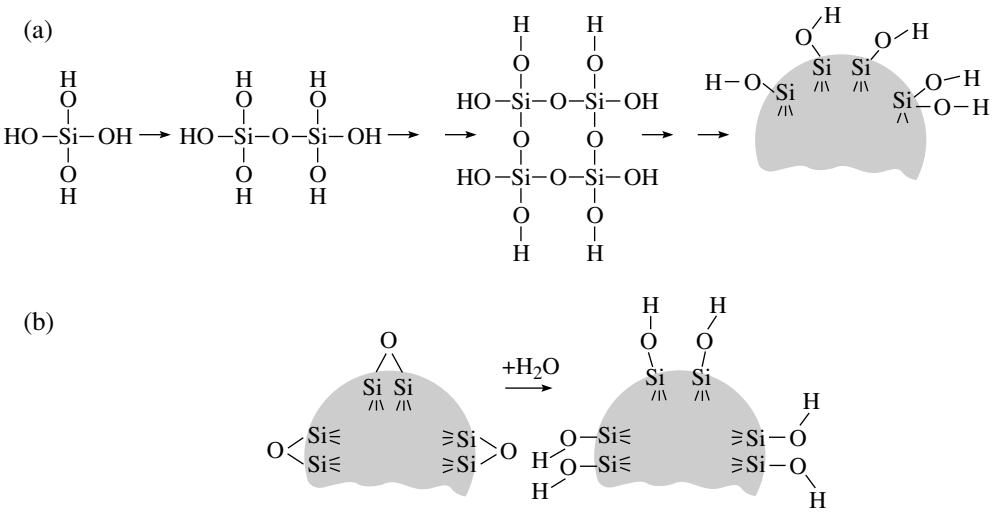

Fig. 1. Schemes of formation of the silica surface structure (≡Si–OH silanol groups) in the course of (a) condensation polymerization and (b) rehydroxylation.

particles and acceleration of their coagulation. As a result, a gel-like material that consisted of a mixture of precipitated silica with snow was formed on the surface. After drying at 105°C, the mixture transformed into a finely dispersed powder. Precipitated silica was removed from the surface and dried with the use of geothermal heat. The density of gel-like silica taken from the snow surface was equal to 2.0 g/cm^3. After drying for 12–16 h at 110°C, the material transformed into a finely dispersed powder, whose density was equal to 0.22–0.24 g/cm^3.

Amorphous silica hydroxylated to different degrees can find wide use in science and engineering [8]. In the general case, ≡Si–OH silanol groups (silanols) are formed on the surface due to the two main thermodynamically favorable processes [8]. First, these groups are formed in the course of synthesis, for example, condensation polymerization of $Si(OH)_4$ (Fig. 1a) when a supersaturated solution of monosilicic acid transforms into polysilicic acids with the subsequent formation of SiO_2 sols and gels containing OH groups on the surface. The final product after drying (xerogel) retains totally or partially silanol groups on the surface. Second, silanol groups can be formed through rehydroxylation of thermally hydroxylated silica upon treatment with water or aqueous solutions (Fig. 1b).

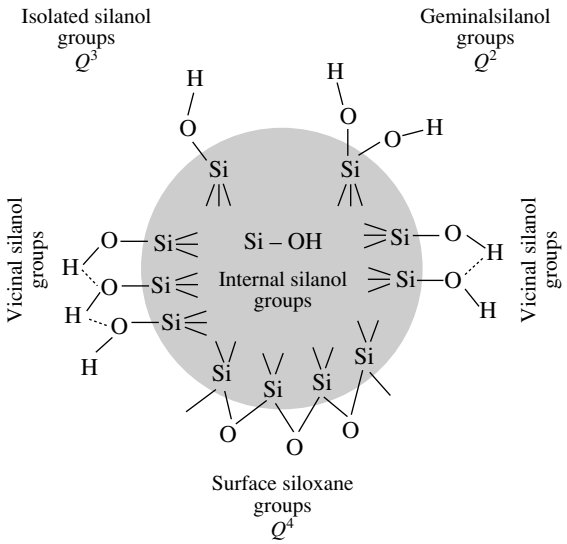

Fig. 2. Types of silanol groups and siloxane bridges on the surface of amorphous silica and internal OH groups.

Different types of groups on the surface and in the bulk of silica are shown in Fig. 2 [8]. These are surface free single (isolated) silanol groups ≡SiOH (Q^3 type); surface free geminal (isolated) silanol or silanediol groups $=Si(OH)_2$ (Q^2 type); vicinal bridging silanol groups, i.e., hydrogen-bonded surface single silanol groups, single geminal groups, and their combinations; ≡Si–O–Si≡ siloxane bridges with the O atom on the surface (Q^4 type); and internal silanol groups located within the skeleton and (or) in very thin ultramicropores of silica. Therefore, amorphous silicas on the surface contain only two main types of OH groups: single and geminal groups, which, in turn, are subdivided into isolated, free, and hydrogen-bonded vicinal silanol groups [8].

The properties of dispersed amorphous silica as an adsorbent are primarily determined by the porous structure and the chemical reactivity of the surface. Note that the chemical reactivity depends on the concentration of OH groups, i.e., on the concentration of all silanol groups and their species, the temperature and energy distribution of silanol groups, and the presence of Si–O–Si siloxane bridges, whereas the surface morphol-

ogy is predominantly governed by the synthesis procedure and the conditions of subsequent treatment of silica. Silanol groups ≡Si–OH can be located on the surface (surface silanols) and in the bulk of amorphous silica particles and (or) in very thin ultramicropores (less than 1 nm in diameter) accessible only for the smallest molecules, for example, water molecules (internal silanols). In [8], it was clearly demonstrated that OH groups on the surface of large transport pores easily, rapidly, and completely enter into the deuterium exchange reaction with D_2O heavy water (introduced in the form of vapor or liquid) at room temperature. However, this process virtually does not involve bound water contained inside the SiO_2 skeleton and isotope exchange with silanol groups in ultramicropores proceeds at a very low rate.

Internal silanol groups (Fig. 2) not responsible for the surface processes are widely occurring species in amorphous silica. The internal silanol groups ≡Si–OH are disregarded when it is necessary to calculate the surface concentration of OH groups (the silanol number α_{OH}, OH/nm^2) and to study the reactive behavior of surface silanol groups, because only the latter groups play a decisive role in different surface processes.

Silanol groups within the skeleton and ultramicropores of silica can be formed in different ways (we consider only a number of them).

(i) For silica prepared by condensation of low-molecular polysilicic acids, individual silanol groups can remain in the inorganic polymer network due to incomplete polycondensation, if this reaction is performed without required partners. Moreover, in silica synthesized from sodium silicate, a number of OH groups can be captured by the silica skeleton during aggregation of primary small-sized particles and then in the course of ageing of the SiO_2 gel.

(ii) According to Iler [4], in the case when colloidal particles are formed through growth in an alkali solution (pH ~ 9), sodium atoms can be adsorbed on particles simultaneously with SiO_2 precipitation. This favors capture of silanol groups by the silica structure.

(iii) In the case of pyrogenic silica, large spherical particles (globules) 10–20 nm in diameter are formed via aggregation of 1–2-nm elementary primary globules produced by hydrolysis in a flame at high temperatures. Since primary particles contain a number of surface silanol groups, these OH groups can be captured inside large globules of the final product.

(iv) Sindorf and Maciel [9] demonstrated that the appearance of internal silanol groups can be explained by diffusion of H_2O molecules inside SiO_2 solid particles (to a depth of 15 nm) at elevated temperatures.

(v) One of the most widespread types of treatment that lead to the formation of silanol groups in the skeleton and ultramicropores of silica is hydrothermal treatment. Hydrothermal treatment of silica species is accompanied by complex processes of dissolution and reprecipitation of silica and water diffusion inside the solid phase. This results in the formation of secondary structurally modified silicas that have pores with a different geometry and can hold silanol groups or bound water within particles and in ultramicropores.

For example, by using hydrothermal treatment in an autoclave at the stage of SiO_2 hydrogels, Doremus [10] prepared a series of silica gels that had a mesoporous structure and a dense packing of particles but did contain ultramicropores. These samples involve silanol groups on the surface and inside silica particles.

With the use of hydrothermal treatment at the xerogel stage, Chertov *et al.* [11] produced silica gels in which particles had different porous (globular, transient, sponge) structures. Similar samples contain silanol groups on the surface and inside silica particles and in ultramicropores.

Upon hydrothermal treatment of initial pyrogenic silicas (aerosils), Gorelik *et al.* [12] synthesized a series of aerosilica gels with different porous structures. Silanol groups on the surface and within silica particles were also contained in these materials.

In [13], modified glasses with different porous structures were prepared by different types of treatments, including long-term boiling of initial porous glasses in water. Apart from surface OH groups, silanol groups were revealed inside particles and in ultramicropores.

It should be expected that internal silanol groups should be contained in different amorphous silicas formed as solid deposits on walls of wells, pipes, and thermal equipment of thermal and electric power stations operating with the use of natural geothermal heat carriers (fields in Russia, New Zealand, Japan, United States, Philippines, Mexico, Iceland, Italy, etc.) [1–3].

The chemical composition of silica sample AK1b prepared in our experiments was as follows (wt %): SiO_2, 81.13; TiO_2, 0.02; Al_2O_3, 0.41; Fe_2O_3, 0.07; FeO, 0.09; MnO, MgO, and CaO, not found; Na_2O, 0.60; K_2O, 0.29; H_2O, 10.93 (drying loss at 105°C); calcination loss at 1000°C, 6.03; and P_2O_5, 0.06 (Σ, 99.63).

The silica dioxide content in the samples after subtraction of losses by drying at 105°C and calcination at 1000°C varied from 95.0–97.69 to 99.02 wt %. The total content of calcium, aluminum, and iron did not exceed 0.6%.

The silica samples precipitated by freezing of the hydrothermal solution had an amorphous structure, as can be judged from the amorphous halo at 0.387–0.40 nm in the X-ray diffraction pattern (Fig. 3a). After calcination at 1000°C, amorphous silica transformed into the crystalline phase with a cristobalite structure (Fig. 3b).

The IR spectra of the precipitated samples were recorded on a Bruker Vector 22/N Fourier-transform IR spectrometer in the wave number range 250–4250 cm^{-1}. The IR spectra in the range 250–1200 cm^{-1} involve three

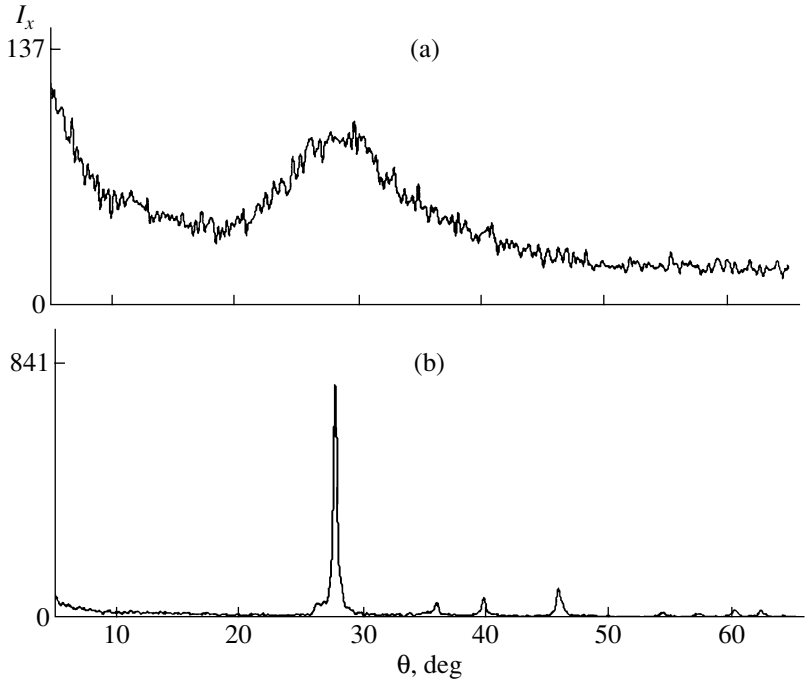

Fig. 3. X-ray powder diffraction patterns of the silica sample (a) before and (b) after calcination at 1000°C.

maxima attributed to the vibrations of Si–O–Si bonds in SiO_2 tetrahedra: two low-intensity maxima at 500 and 750–850 cm^{-1} and one intense maximum at 1096–1104 cm^{-1} (Fig. 4). All the IR spectra in the range 1200–4000 cm^{-1} contain two low-intensity peaks at 1600–1640 and 2344–2368 cm^{-1} and one intense peak at 3440–3480 cm^{-1}. These peaks are associated with the vibrations of hydroxyl groups. However, the band at 3750 cm^{-1} that, according to the data available in the literature, is characteristic of ≡Si–OH free silanol groups was not found in the spectra due to the overlapping with the bands of vicinal silanol groups and, possibly, adsorbed water molecules. The shape of the IR spectra and the location of the two main peaks at 1096–1104 and 3440–3480 cm^{-1} are characteristic of different forms of amorphous silicon dioxide.

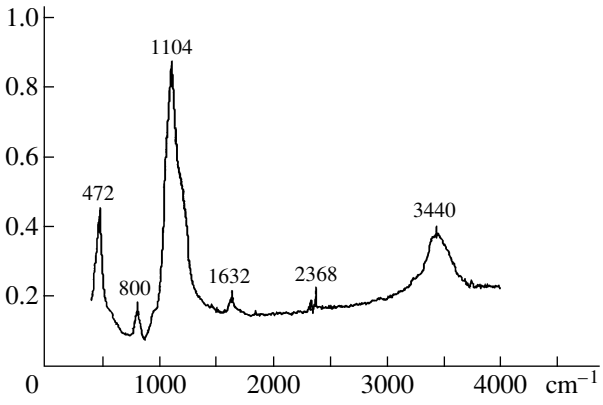

Fig. 4. IR spectrum of the silica sample.

The thermal analysis of silica sample AK1b was performed on a Perkin-Elmer Pyris Diamond TG/TGA thermal analyzer (heating rate, 20 K/min) in air (Fig. 5).

The optical reflectances of the dispersed silica surface were measured with an MSFU-K microscope spectrophotometer in the wavelength range 400.0–760.0 nm. The optical reflectance (whiteness) for the geothermal silica samples varied from 91–95 to 94–98%. As the wavelength increases, the reflectance increases in the following way: 480.0 nm, 0.9402; 500.0 nm, 0.9531; 520.0 nm, 0.95029; 540.0 nm, 0.95394; 560.0 nm, 0.96534; 580.0 nm, 0.96592; 600.0 nm, 0.97425; 620.0 nm, 0.97911; 640.0 nm, 0.97679; 660.0 nm, 0.97182; 680.0 nm, 0.97274; and 700.0 nm, 0.98265.

The surface area and volume of pores in the silica samples were determined using a Micrometrics ASAP-2010N porosity analyzer (USA) from the data on low-temperature nitrogen adsorption. The method is based on the measurement of the nitrogen adsorption isotherms at the liquid-nitrogen temperature [14]. In the course of experiments, the change in the weight of the dispersed sample was measured and used to determine the amount of adsorbed nitrogen at a specific relative pressure of nitrogen P/P_0 in a cell with the sample (P is the nitrogen pressure in the system, P_0 is the nitrogen

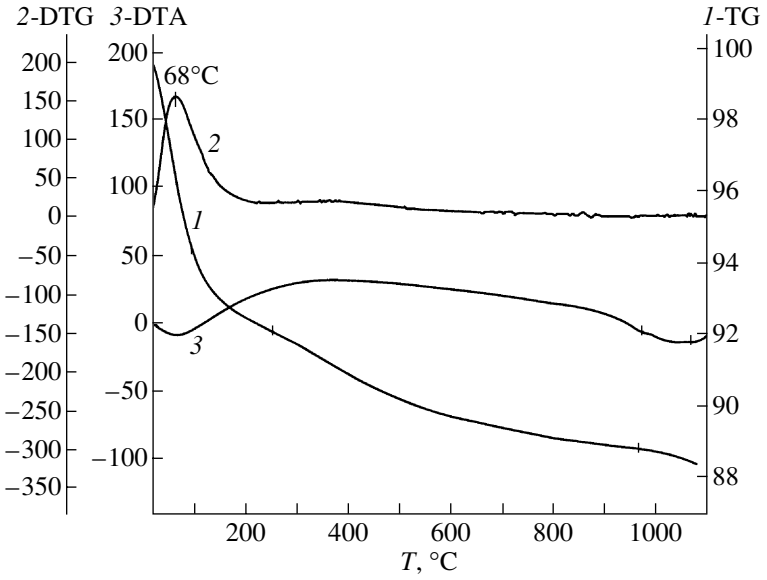

Fig. 5. (*1*) Thermogravimetric, (*2*) differential thermogravimetric, and (*3*) DTA curves for the silica sample.

saturation vapor pressure at a given temperature). The volume V of adsorbed nitrogen was determined initially with a sequential increase in the relative pressure P/P_0 from 0.01 to 1.0 (adsorption curve) and then with a decrease in the relative pressure P/P_0 from 1.0 to 0.04 (desorption curve). The dependence $V(P/P_0)$ for silica sample AK1b is plotted in Fig. 6.

The experimental curves obtained belong to adsorption isotherms of the IV type [14]. The curves are convex in the vicinity of zero, become concave after passing through an inflection point at $P/P_0 = 0.3$–0.5, and are again convex in the vicinity of $P/P_0 = 1.0$ (Fig. 6).

The specific surface was determined by the Brunauer–Emmett–Teller (BET) and Brunauer–Deming–Halsey (BDH) methods. The specific surface was calculated using the Brunauer–Emmett–Teller equation for polymolecular adsorption of vapor from the experimental data obtained in the range of the relative pressures $P/P_0 = 0.0$ –1.0 [14].

RESULTS AND DISCUSSION

Within the classical theory of adsorption and desorption [14], the determined dependences $V(P/P_0)$ were used to calculate the differential distributions of volumes V_p and surfaces S_p of pores with diameters d_p in a specific range and also the total volumes and total surfaces of pores with diameters from 1.7 nm to a given diameter d_p. Furthermore, we calculated the differential dependences $dV_p/d\log(d_p)$ and $dS_p/d\log(d_p)$. The curves $dV_p/d\log(d_p)$ and $dS_p/d\log(d_p)$ exhibit maxima at d_p = 18.0 and 11.7 nm, respectively.

The pore parameters obtained by the adsorption method for the samples of dispersed geothermal silica are listed in Table 1. The designations in Table 1 are as follows: volumes 1 and 2 (used for calculations of coefficients) are the cell volumes automatically measured by the instrument at room temperature and after dipping in a Dewar vessel with liquid nitrogen, respectively; S_S is the specific determined at the fixed relative pressure $P/P_0 = 0.200$; S_{BET} is the total specific surface of pores according to the BET method; S_{MP} is the specific surface of micropores with a diameter of an order of 1.7 nm; S_{AC} is the total specific surface determined

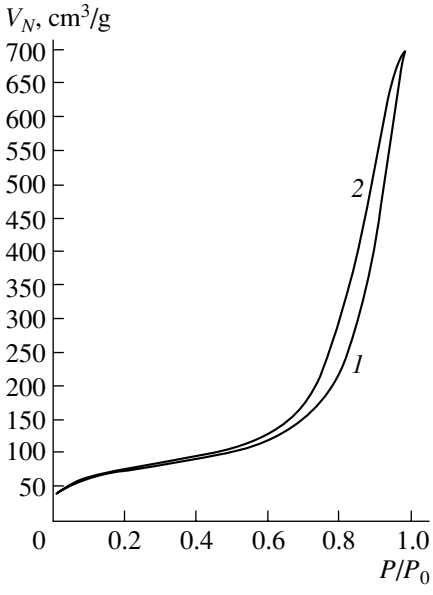

Fig. 6. Nitrogen (*1*) adsorption and (*2*) desorption curves for the silica sample.

Table 1. Sizes, specific surfaces, and volumes of pores in samples of finely dispersed geothermal silica

Temperature, K	77.2
Pressure P_0, mmHg	747.17
Sample weight, g	0.13
Volume 1, cm^3	17.45
Volume 2, cm^3	54.32
S_S, m^2/g	263.53
S_{BET}, m^2/g	274.64
S_{MP}, m^2/g	26.33
S_{AC}, m^2/g	260.25
S_{DC}, m^2/g	333.52
V_S, cm^3/g	0.871
V_{MP}, cm^3/g	0.00827
V_{AC}, cm^3/g	1.078
V_{DC}, cm^3/g	1.088
d_{BET}, nm	12.692
d_A, nm	16.575
d_D, nm	13.058

by the BDH method from the adsorption curve for pores with diameters from 1.7 to 300.0 nm (the BDH surface area); S_{DC} is the specific surface determined by the BDH method from the desorption curve for pores with diameters from 1.7 to 300.0 nm; V_S is the total volume of pores with diameters smaller than 40.0 nm at the fixed relative nitrogen pressure $P/P_0 = 0.950$; V_{MP} is the volume of micropores with a diameter of an order of 1.7 nm; V_{AC} is the total volume determined by the BDH method from the adsorption curve for pores with diameters from 1.7 to 300.0 nm (the BDH volume); V_{DC} is the total volume determined by the BDH method from the desorption curve for pores with diameters from 1.7 to 300.0 nm; $d_{BET} = 4V_S/S_{BET}$ is the mean pore diameter; $d_A = 4V_{AC}/S_{AC}$ is the mean pore diameter calculated from the volume and specific surface determined by the BDH method from the adsorption curve; and $d_D = 4V_{DC}/S_{DC}$ is the mean pore diameter calculated from the volume and specific surface determined by the BDH method from the desorption curve.

It can be seen from the data presented in Table 1 that, for silica sample AK1b prepared from the solution of wells of the Mutnovsk field, the specific surface is as large as 300 m^2/g, the porosity is equal to 1.1 g/cm^3, and the mean pore diameter lies in the range 12.7–16.6 nm. The specific surface and volume of micropores in the geothermal silica samples appear to be relatively small. The ratio between the specific surface of micropores and the total specific surface of pores falls in the range 0.09–0.107, and the ratio of the micropore volume to the total pore volume is even smaller (0.005–0.0085).

The specific surfaces and volumes of pores as a function of their diameter are given in Table 2. As can be seen from this table, the diameters of pores in sample AKb1 of geothermal silica lie in a narrow range. The differential distribution of volumes over pore diameters exhibits a maximum at $d_p = 33$ nm, and the differential distribution of surfaces over pore diameters has two close approximately identical maxima at 13 and 9 nm. Pores with diameters in the ranges $d_p = 5.18$–20.61 nm, $d_p = 5.18$–26.47 nm, and $d_p = 5.18$–40.00 nm occupy 71.1, 79.8, and 88.3% of the total volume, respectively. In turn, pores with diameters in the ranges $d_p = 5.18$–26.47 nm and $d_p = 5.18$–40.00 nm account for 60.9 and 76.4% of the total specific surface. These pore parameters provide a sufficiently high reactivity of the precipitated material and rapid homogeneous complete dissolution of silica in technological processes.

Knowing the specific surface of silica S_{BET} (m^2/g) and the weight percent Δm_{H_2O} (wt %), i.e., the total mass loss due to removal of water and OH groups in the course of thermogravimetric analysis, it is possible to determine the total concentration δ_{OH} (OH/nm^2) of all silanol groups on the surface and in the bulk of silica per unit specific surface of sample AK1b; that is,

$$\delta_{OH} = (\Delta m_{H_2O} \cdot 2 \cdot 6.02 \times 10^3)/(18 S_{BET}). \quad (3)$$

By setting $S_{BET} = 300$ m^2/g, assuming that the temperature of complete removal of all silanol groups is equal to 1000°C, and taking into account the thermogravimetric data, we calculated the total concentrations δ_{OH} (on the surface and in the bulk) per specific surface of the sample at different temperatures (Table 3).

Many researchers have investigated different aspects of dehydroxylation and rehydroxylation of amorphous silica surfaces. This is explained by the fact that their chemical properties, which are predominantly determined by the concentration, distribution, and reactivity of surface silanol groups ≡Si–OH, are of crucial theoretical and practical importance.

The dependences of the silanol number $\alpha_{OH,T}$ for the surface on the temperature T_{PHT} of preliminary heat treatment under vacuum according to the deuterium exchange data (the subscript T indicates the total silanol number without separating into isolated free, geminal free, and vicinal OH groups) are presented in Fig. 7 and Table 3. This dependence for different SiO_2 samples allows us to determine the Zhuravlev physicochemical constants [the silanol number $\alpha_{OH,T}$, the degree of coverage $\theta_{OH,T}$ of the SiO_2 surface by OH groups at different heat treatment temperature T_{PHT} (°C)], which are widely used in the world scientific literature. The dependence of the silanol number $\alpha_{OH,T}$ was obtained using 100 samples of amorphous silicas of nine different types, whose specific surfaces S_{Kr} (determined by the BET method from the data on the low-temperature krypton adsorption) and diameters of accessible pores

Table 2. Volumes and specific surfaces of pores as a function of their diameter for the geothermal silica sample according to the adsorption analysis data

Pore diameter d_p, nm	Mean diameter, nm	Porosity, g/cm^3	Total porosity, g/cm^3	Specific surface of pores, m^2/g	Total specific surface of pores, m^2/g
333.0–125.1	150.03	0.0238	0.0238	0.635	0.635
125.1–88.9	100.89	0.0333	0.0571	1.321	1.956
88.9–72.7	79.1	0.0284	0.0856	1.438	3.394
72.7–40.0	47.2	0.1539	0.2395	13.03	16.42
40.0–26.5	30.4	0.1669	0.4065	21.94	38.37
26.5–20.6	22.7	0.1303	0.5368	22.90	61.27
20.6–16.7	18.2	0.1182	0.6550	25.93	87.20
16.7–14.0	15.1	0.0960	0.7510	25.35	112.55
14.0–11.6	12.6	0.1005	0.8516	31.89	144.45
11.6–10.3	10.89	0.0550	0.9066	20.23	164.68
10.3–8.36	9.11	0.0764	0.9831	33.57	198.25
8.36–7.00	7.55	0.0425	1.0257	22.55	220.80
7.00–5.97	6.40	0.0243	1.0501	15.25	236.06
5.97–5.18	5.52	0.0141	1.0642	10.24	246.310
5.18–4.54	4.81	0.0079	1.0722	6.624	252.93
4.54–4.02	4.24	0.0039	1.0761	3.760	256.69
4.02–3.58	3.77	0.0011	1.0773	1.226	257.92
3.58–3.20	3.36	0.000061	1.0774	0.072	257.99
3.20–1.96	2.01	0.000059	1.0774	0.118	258.11
1.96–1.86	1.91	0.00046	1.0779	0.963	259.07
1.86–1.76	1.81	0.00053	1.0784	1.178	260.25

Table 3. Concentrations of OH groups on the surface and in the bulk of hydrothermally treated silica sample AK1b (as a function of temperature)

Number of OH groups per unit specific surface of silica, OH/nm^2	Temperature of preliminary heat treatment, °C							
	200	300	400	500	600	700	800	900
δ_{OH}	8.29	6.71	4.92	3.33	2.23	1.49	0.89	0.40
α_{OH}	4.90	3.56	2.33	1.84	1.52	1.30	0.70	0.40
γ_{OH}	3.39	3.15	2.59	1.49	0.71	0.19	0.19	0.0

Note: δ_{OH} is the total concentration of silanol groups (according to the water loss), α_{OH} is the concentration of silanol groups on the SiO_2 surface, and γ_{OH} is the concentration of silanol groups inside the skeleton and micropores of the sample.

varied over very wide ranges from 9.5 to 945 m^2/g and from ~1 to 1000 nm and more, respectively.

Although the quantities S_{Kr} and d (without regard for ultramicropores) for different SiO_2 samples differ substantially, their silanol numbers $\alpha_{OH,\,T}$ at a specific temperature of preliminary heat treatment are close to each other and decrease in a similar manner under close heating conditions. The silanol number $\alpha_{OH,\,T}$ decreases rapidly in the range 190–400°C (portion *AB* in Fig. 7) and then changes more slowly in the range from 400 to ~780°C (portion *BC* in Fig. 7), in which the curve becomes more flattened. The dashed lines bound the region of scatter in the experimental data observed for different SiO_2 samples over the entire temperature range from 190 to ~780°C. Table 4 presents the Zhuravlev physicochemical constants [4] (corresponding to the solid lines in Fig. 7), i.e., the most probable silanol numbers $\alpha_{OH,\,T}$ or the concentrations of surface silanol groups (Table 4, column 2) at fixed temperatures T_{PHT} (°C) of preliminary heat treatment (Table 4, column 1). The corresponding averaged degrees of surface coverage $\theta_{OH,\,T}$ by OH groups are also listed in Table 4 (column 3). The physicochemical constants $\alpha_{OH,\,T}$ and

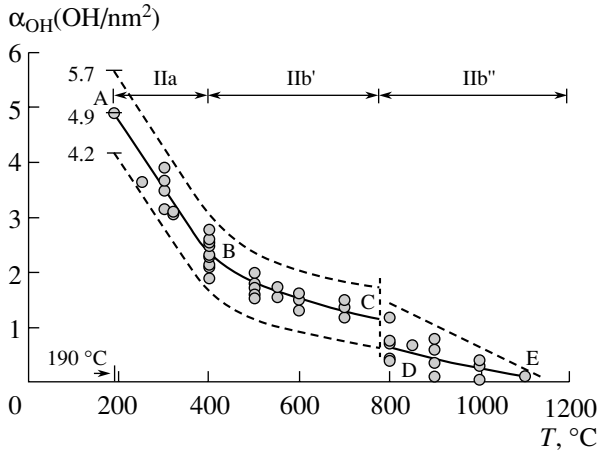

Fig. 7. Dependence of the silanol number $\alpha_{OH} = \alpha_{OH,\,T}$ on the temperature T_{PHT} of preliminary heat treatment for 16 different SiO_2 samples. $\alpha_{OH,\,T}$ = 4.9 OH/nm^2 (left upper point) corresponds to the surface hydroxylated to a maximum degree. Dashed lines bound the region of the experimental data. Range *II* at T_{PHT} > 190°C is divided into subranges *IIa* (190–400°C) and *IIb*' (400–780°C) in which portions *AB* and *BC* have different slopes. For explanation of portion *DE* in subrange *IIb*" (800–1200°C), see the text.

$\theta_{OH,\,T}$ are universal constants for any amorphous silicas irrespective of their origin and structural characteristics (Table 4, columns 1–3; Fig. 7, portions *AB*, *BC*) if they in the initial state have a completely hydroxylated surface (Fig. 7, point *A*). In this case, a possible presence of silanol groups in the bulk and ultramicropores is ignored.

The dependences $\alpha_{OH,\,T} = f(T, C)$ and $\theta_{OH,\,T} = g(T, C)$ in range *II* (Fig. 7) have two portions with different slopes in range *IIa* from 190 to ~400°C (straight solid line) and range *IIb*' (solid line approximated by a power law). Portion *AB* (Fig. 7) can be approximated by the linear relationship with the use of reference point *A* ($\alpha_{OH,\,T}$ = 4.9, Table 4); that is,

$$\alpha_{OH,\,T}\,(\text{OH/nm}^2) = -0.0122 \cdot T(^\circ\text{C}) + 7.218, \qquad (4)$$

whose approximation reliability R^2 = 0.8768 is close to unity.

Portion *BC* (Fig. 7) can be approximated by the power relationship with the use of reference point *B* ($\alpha_{OH,\,T}$ = 2.33, Table 4); that is,

$$\alpha_{OH,\,T}\,(\text{OH/nm}^2) = 1155.6 \cdot T(^\circ\text{C})^{-1.0367}, \qquad (5)$$

whose approximation reliability is R^2 = 0.8516.

The condensation of silanols

$$(\equiv\text{Si–OH}) + (\equiv\text{Si–OH}) \longrightarrow \longrightarrow (\equiv\text{Si–O–Si}\equiv) + \text{H}_2\text{O}\uparrow \qquad (6)$$

has been studied in detail by Zhuravlev with colleagues and also in works of other authors. This reaction occurs at temperatures corresponding to ranges *IIa*, *IIb*', and *IIb*", even though the activation energies E_D of thermal desorption in these ranges differ substantially [4]. In the case when the degree of surface coverage by silanol groups is high $1 \geq \theta_{OH,\,T} > 0.5$ (range *IIa*, Table 4), the activation energy E_D of thermal desorption can be represented by the empirical expression [4]

$$E_D = 31.4 - 12.3\theta_{OH,\,T}, \qquad (7)$$

where the activation energy E_D varies weakly in the narrow range 19–25 kcal/mol. To put it differently, the activation energy E_D almost does not depend on the concentration of silanol groups and is predominantly governed by the disturbances of surface OH groups linked together through hydrogen bonds. Note that these disturbances are suppressed upon disappearance of this type of vicinal silanol groups at ~400°C (at $\theta_{OH,\,T}$ ~0.5). Therefore, at temperatures in range *IIa* (portion *AB* in Fig. 7), there are hydrogen bonds (lateral interactions) between neighboring vicinal OH groups when their degree of coverage is high.

If the degree of surface coverage by OH groups ($\theta_{OH,\,T} < 0.5$, range *IIb*'), the main contribution to portion *BC* is made by free single OH groups, free geminal OH groups, and SiOSi bridges (Figs. 2, 7). In ranges *IIb*' and *IIb*", the activation energy *ED* increases drastically from 25 to 50 kcal/mol and higher with a decrease in the silanol number $\alpha_{OH,\,T}$. When there are only free OH groups surrounded by SiOSi bridges, these bridges can occupy relatively large surface areas due to the high-temperature activation of silica. Under these conditions, the main mechanism responsible for the transfer of OH groups necessary for the condensation reaction (6) can be represented by disordered migration of protons along the surface (activated surface diffusion of OH groups). The final stage involves the release of the water molecule owing to the interaction of two OH groups, which accidentally come close together to a distance of ~0.3 nm (characteristic hydrogen bond length). At a low concentration of OH groups (Fig. 7, portions *BC*, *DE*), the condensation reaction (6) is limited by proton diffusion along the SiO_2 surface.

At temperatures corresponding to portion *DE* (Fig. 7), geminal groups are completely absent and the condensation reaction is limited by the interaction of widely spaced free single OH groups. In this high-temperature range (Fig. 7, portion *DE*), amorphous silica can transform partially or completely into a crystalline silica modification. A similar transformation of amorphous sample AK1b (prepared by precipitation of the hydrothermal solution) into the crystalline phase with a cristobalite structure at 1000°C was observed in the present work (Figs. 3a, 3b). Therefore, portion *DE* in Fig. 7 is difficult to approximate with a sufficient reliability, and only averaged silanol numbers $\alpha_{OH,\,T}$ are presented in Table 4.

Under the assumption that, according to the above results, the maximum concentration of surface OH

groups in silicas of different types at a temperature of 190° (in the range 180–200°C) is equal to 4.9 OH/nm^2, the concentration γ_{OH} (OH/nm^2) of internal silanol groups OH (internal water) per unit specific surface in sample AK1b can be determined as the difference

$$\gamma_{OH}(T) = \delta_{OH}(T) - \alpha_{OH}(T). \quad (8)$$

The results of calculations from relationship (8) are given in Table 3. These data represent the temperature dependences of the concentrations of OH groups on the surface and in the bulk of silica sample AKb1. The dependences of the concentrations δ_{OH}, α_{OH}, and γ_{OH} on the temperature T (°C) of preliminary heat treatment are plotted in Fig. 8. At a temperature of 200°C, the concentrations of surface and internal OH groups in silica precipitated from the hydrothermal solution are comparable in magnitude. In the range 200–400°C, internal water is slowly removed and the concentration γ_{OH} decreases insignificantly with an increase in the temperature. Since the removal rate of internal water is relatively low, the concentration of internal OH groups becomes equal to the concentration of surface OH groups at temperatures in the range 375–425°C and somewhat exceeds the latter concentration at a temperature of approximately 400°C, as can be judged from the intersection of the dependences $\gamma_{OH}(T)$ and $\alpha_{OH}(T)$ in Fig. 8.

At temperatures higher than 400°C, the removal rate of internal water becomes higher: the concentration of internal OH groups at 600°C is lower than that of surface OH groups by a factor of more than two. The curves $\delta_{OH}(T)$ and $\alpha_{OH}(T)$ in Fig. 8 intersect at a temperature of approximately 900°C. This suggests that internal OH groups exist in silica sample AKb1 at high temperatures. Internal OH groups are completely removed at temperatures of 900–1000°C, when the concentration of surface OH groups becomes considerably lower than an initial concentration of 4.6–4.9 OH/nm^2. In the temperature range 400–800°C, the experimental concentrations γ_{OH} (OH/nm^2), which correspond to the water content in the bulk of the silica sample precipitated from the hydrothermal solution, can be approximated by the relationship

$$\ln\gamma_{OH}(T) = 0.943 - 0.0065(T^2 - 673^2). \quad (9)$$

The data obtained indicate that the mechanisms of water removal from the surface and bulk of the sample differ fundamentally. As the temperature T increases, the silanol number $\alpha_{OH}(T)$ decreases rapidly in the range 200–400°C and changes more slowly at temperatures above 400°C because of the disappearance of surface vicinal silanol groups. By contrast, the concentration $\gamma_{OH}(T)$ decreases slowly in the range 200–400°C and the removal rate of internal OH groups increases in the temperature range 400–600°C. In our opinion, this difference can be explained by the fact that, first, condensation (6) of silanol groups in the case of internal water proceeds in the bulk rather than on the surface and, second, the removal of internal water requires the transfer of water molecules from the bulk of particles to their surface. The transfer of H_2O molecules can be provided by diffusion through the bulk of particles or ultramicropores. The diffusion rate increases with an

Table 4. Concentrations of surface silanol groups $\alpha_{OH,T}$ and degrees of surface coverage $\theta_{OH,T}$ by OH groups (Zhuravlev physicochemical constants [4]) as a function of the temperature T of preliminary heat treatment under vacuum for different samples of amorphous silicas

Temperature of preliminary heat treatment under vacuum T, °C	Concentration of surface silanol groups $\alpha_{OH,T}$, OH/nm^2	Degree of coverage of the silica surface by OH groups $\theta_{OH,T}$
Portion *AB* (approximated by the linear equation, Fig. 7)		
190	4.90	1.00
225	4.47	0.91
250	4.17	0.85
275	3.86	0.79
300	3.56	0.73
325	3.25	0.66
350	2.95	0.60
375	2.64	0.54
400	2.33	0.48
Portion *BC* (approximated by the power equation, Fig. 7)		
425	2.18	0.44
450	2.05	0.42
475	1.94	0.40
500	1.84	0.38
525	1.75	0.36
550	1.67	0.34
575	1.59	0.32
600	1.52	0.31
625	1.46	0.30
650	1.40	0.29
675	1.35	0.28
700	1.30	0.27
725	1.25	0.26
750	1.21	0.25
775	1.17	0.24
Portion *DE* (from 800 to 1200°C, see Fig. 7 and text)		
800	0.70	0.14
900	0.40	0.08
1000	0.25	0.05
1100	0.15	0.03
1200	0.0	0.0

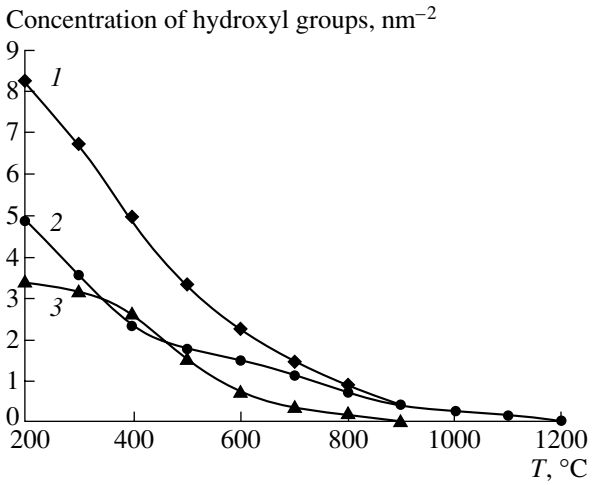

Fig. 8. Temperature dependences of the concentrations of hydroxyl groups (*1*) δ_{OH}, (*2*) α_{OH}, and (*3*) γ_{OH} (see Table 3).

increase in the temperature. This leads to an increase in the slope of the curve $\gamma_{OH}(T)$ in the range 400–600°C.

CONCLUSIONS

A comparison of the temperature dependence of the concentration $\delta_{OH}(T)$ determined from the thermogravimetric data for a silica sample precipitated from a hydrothermal solution with the Zhuravlev physicochemical constants $\alpha_{OH}(T)$ demonstrated that the concentration of internal OH groups at a temperature of 200°C is considerable and comparable to the concentration of surface OH groups. Thus, the performed investigation revealed a new type of amorphous silica with a high concentration of internal silanol groups. This type is represented by silica samples prepared by coagulation and precipitation of colloidal silica particles from the hydrothermal solution or silica formed through deposition of colloidal particles from the flow of a hydrothermal solution to walls of carrying channels.

The conclusion was drawn that a considerable concentration of internal water in silica precipitated from the hydrothermal solution is explained by two factors: (1) the mechanism of formation of colloidal particles via polycondensation of orthosilicic acid molecules and the presence of noncompensated regions in the inorganic polymer network and (2) the effect of the aqueous solution at elevated temperatures and pressures (equivalent to hydrothermal treatment resulting in dissolution and reprecipitation of silica) and water diffusion.

The analysis of the dependences $\alpha_{OH}(T)$ and $\gamma_{OH}(T)$ for silica precipitated from the hydrothermal solution indicated that the mechanisms of removal of internal and surface water differ fundamentally. The removal rate of internal water is low in the temperature range 200–400°C and increases at temperatures of 400–600°C. This difference can be associated with the fact that internal water is removed as a result of condensation of silanol groups in the bulk of particles or ultramicropores and the condensation products are transferred to the particle surface due to molecular diffusion whose rate increases with an increase in the temperature.

REFERENCES

1. Potapov, V.V., Precipitation of Amorphous Silica from a High-Temperature Hydrothermal Solution, *Fiz. Khim. Stekla*, 2004, vol. 30, no. 1, pp. 101–111 [*Glass Phys. Chem.* (Engl. transl.), 2004, vol. 30, no. 1, pp. 73–81].
2. Potapov, V.V., Formation of Solid Deposits of Amorphous Silica in a Flow of Hydrothermal Solution, *Fiz. Khim. Stekla*, 2004, vol. 30, no. 1, pp. 112–121 [*Glass Phys. Chem.* (Engl. transl.), 2004, vol. 30, no. 1, pp. 82–89].
3. Potapov, V.V., *Kolloidnyi kremnezem v gidrotermal'nom rastvore* (Colloidal Silica in Hydrothermal Solution), Vladivostok: Dal'nauka, 2003.
4. Iler, R.K., *The Chemistry of Silica*, New York: Wiley, 1979. Translated under the title *Khimiya kremnezema*, Moscow: Mir, 1982.
5. Chukhrov, F.F., *Kolloidy v zemnoi kore* (Colloids in Crust), Moscow: Akad. Nauk SSSR, 1955.
6. Lebedev, L.M., *Metakolloidy in endogennykh mestorozhdeniyakh*, (Metacolloids in Endogenic Fields), Moscow: Nauka, 1965.
7. Potapov, V.V., Physicochemical Processes During Precipitation of Silica from a Hydrothermal Solution, *Teor. Osn. Khim. Tekhnol.*, 2004, vol. 38, no. 1, pp. 77–85.
8. Zhuravlev, L.T., The Surface Chemistry of Amorphous Silica: Zhuravlev Model, *Colloids Surf., A*, 2000, vol. 173, pp. 1–38.
9. Sindorf, D.W. and Maciel, G.E., Study of Silica Gel Using Trimethylsilane Bonding as a Probe of Surface Geometry and Reactivity, *J. Phys. Chem.*, 1982, vol. 86, pp. 5208–5219.
10. Doremus, R.H., *J. Phys. Chem.*, 1971, vol. 75, pp. 3147–3148.
11. Chertov, V.M., Dzhambaeva, D.B., Plachinda, A.S., and Neimark, I.E., Hydroxyl Groups on Surface and inside Globules of Silica Gels Prepared from Hydrothermally Treated Hydrogels, *Zh. Fiz. Khim.*, 1966, vol. 40, pp. 520–525.
12. Gorelik, R.L., Zhuravlev, L.T., Kiselev, A.V., Nikitin, Yu.S., Oganesyan, E.B., and Shengeliya, K.Ya., Investigation into the Mechanism of Formation of Utraporosity in Silica Gels during Hydrothermal Treatment, *Kolloidn. Zh.*, 1971, vol. 33, pp. 51–58.
13. Gorelik, R.L., Zhdanov, S.P., Zhuravlev, L.T., Kiselev, A.V., Luk'yanovich, V.M., Malikova, I.Ya., Nikitin, Yu.S., and Sheshenina, Z.E., The Influence of Thermal and Hydrothermal Treatment on the Pore Structure in Porous Glasses, *Kolloidn. Zh.*, 1973, vol. 35, pp. 911–917.
14. Gregg, S.J. and Sing, K.S.W. *Adsorption, Surface Area, and Porosity*, New York: Academic, 1982, 2nd ed. Translated under the title *Adsorptsiya, udel'naya poverkhnost', poristost'*, Moscow: Mir, 1984.

SPELL: OK